Carbohydrate Polymers 83 (2011) 130–136

Contents lists available at ScienceDirect

Carbohydrate Polymers

journal homepage: www.elsevier.com/locate/carbpol

The preparation and characterization of a novel amphiphilic oleoyl-carboxymethyl chitosan self-assembled nanoparticles

Yanyan Li [a,*], Shanshan Zhang [a], Xiangjun Meng [a], Xiguang Chen [b], Guodong Ren [a]

[a] College of Life Sciences, HeBei University, 180# East Wusi Road, Baoding 071002, People's Republic of China
[b] College of Marine Life Science, Ocean University of China, People's Republic of China

ARTICLE INFO

Article history:
Received 14 May 2010
Received in revised form 30 June 2010
Accepted 15 July 2010
Available online 21 July 2010

Keywords:
Oleoyl-carboxymethyl chitosan
Solubility
Biocompatibility
Self-aggregation nanoparticles
Rifampicin

ABSTRACT

Oleoyl-carboxymethyl chitosan (OCMCS) was synthesized by reacting carboxymethyl chitosan (CMCS) with oleoyl chloride. The FT-IR spectra suggested the formation of an amide linkage between amino groups of CMCS and oleoyl chloride. The solubility property of OCMCS was similar with CMCS. The CS was insoluble while the OCMCS and CMCS could be soluble at neutral pH. The improvement of solubility made CS have a wide range of uses in the biotechnology and pharmaceutical fields. All the CS, CMCS, and OCMCS had good biocompatibility based on the results of the erythrocyte toxicity assay. Formation of self-aggregation was observed by use of pyrene as a fluorescent probe in the OCMCS aqueous solution. Nanoparticles were prepared using an o/w emulsification method. The OCMCS nanoparticles were more regular and compact than OCS nanoparticles we prepared previously. Mean diameter of the OCMCS nanoparticles was 161.8 nm. Rifampicin, as a model drug, was investigated for the release properties of OCMCS nanoparticles in vitro. The addition of crosslinker sodium tripolyphosphate (STPP) could slower the release of rifampicin. The rifampicin release rate was sensitive to the pH of the release media.

1. Introduction

Amphiphilic copolymers consisting of hydrophilic and hydrophobic segments can form micelles structures with the hydrophobic inner core and the hydrophilic outer shell in aqueous media. These polymeric nanoparticles exhibit unique characteristics, depending on hydrophobic/hydrophilic constituents, such as unusual rheological features, a nanoscale hydrodynamic radius with core–shell structure, and thermodynamic stability (Kakizawa, Harada, & Kataoka, 2001). The aggregation of amphiphilic polymers is of growing interest with respect to biological importance and pharmaceutical or biotechnological applications (Kim et al., 2006). The polymeric micelles have the ability to take water insoluble drugs or low molecular weight organic compounds and disperse them in the aqueous solution (Koziara, Whisman, Tseng, & Mumper, 2006). Longer hydrophilic chains and bigger hydrophobic groups help stabilize the micelle structure and protect drug compounds from the environment.

Chitosan, α-(1–4)-2-amino-2-deoxy-β-D-glucan, is a deacetylated form of chitin, an abundant natural polysaccharide present in crustacean shells. Its unique characteristics such as positive charge, biodegradability, biocompatibility, nontoxicity, and rigid linear molecular structure make this macromolecule ideal as a drug carrier and delivery material (Gupta & Jabrail, 2006; Li, Liu, & Yao, 2002). Chitosan molecules have no amphiphilic property and cannot form micelles in water. Thus, there had many reports on hydrophobic modifications of chitosan, such as palmitoyl glycol chitosan (Martin et al., 2002), deoxycholic acid-modified chitosan (Kim, Gihm, & Park, 2001), linoleic acid-modified chitosan (Chen, Lee, & Park, 2003), linolenic acid-modified chitosan (Liu, Desai, Chen, & Park, 2005), *N*-alkyl-*O*-sulphate chitosan (Zhang, Ping, Zhang, & Shen, 2003), chitosan–polylactide graft copolymer (Wu et al., 2005), etc. Recently, water-soluble chitosan derivatives had been used to increase their stability in biological solution and decrease the cytotoxicity induced by acidic solution (Garcia-Fuentes, Prego, Torres, & Alonso, 2005; Park et al., 2006; Xu & Du, 2003). CMCS is emerging as a novel carrier of drugs because of its solubility in water and biocompatibility. But there had only few reports on using CMCS to prepare nanoparticles (Liu et al., 2007).

In our previous work, our research group had prepared linoleic acid-modified chitosan nanomicelles and oleoylchitosan nanoparticles (Li et al., 2007). But most of these products were insoluble in biological solution. Thus, it was expected that the introduction of hydrophilic group to chitosan would improve soluble behavior in the aqueous solution. Herein, we introduce both hydrophilic group carboxymethyl and hydrophobic oleoyl to chitosan to get a water-soluble amphiphilic polymer.

* Corresponding author. Tel.: +86 0312 5079364; fax: +86 0312 5079364.
E-mail address: liyanyan203@hotmail.com (Y. Li).

0144-8617/$ – see front matter © 2010 Elsevier Ltd. All rights reserved.
doi:10.1016/j.carbpol.2010.07.030

In this paper, OCMCS was synthesized by reacting CMCS with oleoyl chloride. The chemical structures of these polymers were characterized by FT-IR. The effects of structure of the OCMCS amphiphilic derivatives on solubility and the formation of nanoparticle were carried out. OCMCS nanoparticles were prepared by an o/w emulsification method. Hydrophobic drug rifampicin was selected as model drug. The drug release profile from the OCMCS nanoparticles was investigated by changing the pH of release media, as well as concentration of crosslinker STPP to evaluate the potential of the loaded nanoparticles as delivery system.

2. Experiment

2.1. Materials

Chitosan, degree of deacetylation 82%, molecular weight 38 kDa, was made from crab shell and obtained from Biotech Co. (Mokpo, Korea). Pyrene, oleoyl chloride, pyridine, chloroform, methylene chloride, monochloroacetic acid were purchased from Sigma Chemicals. Rifampicin was kindly donated by the Jiangbei Pharmaceutical Factory (Zhejing, China).

2.2. Synthesis of OCMCS

The OCMCS was synthesized via two reaction steps: (1) the preparation of CMCS and (2) conjugation of oleoyl and CMCS.

CMCS was prepared by the method of Liu, Guan, Yang, Li, and Yao (2001). CS (1 g), sodium hydroxide (1.2 g), isopropanol (4 ml) and water (5 ml) were added into a flask (50 ml) to swell and alkalize at a given temperature for 1 h. The monochloroacetic acid (1.0 g) was dissolved in isopropanol (2 ml), and added into the reaction mixture dropwise for 30 min and reacted for 3 h at the same temperature, then stopped by adding 70% ethyl alcohol. The solid was filtered and rinsed in 70–90% ethyl alcohol to desalt and dewater.

OCMCS was synthesized by reacting CMCS with oleoyl chloride using the method we used to prepare OCS previously. CMCS (1.0 g) was soaked in a mixture of pyridine (30 ml) and chloroform (15 ml) for one day. The oleoyl chloride dissolved in chloroform (5 ml) was added dropwise for 1 h. The mixture was then stirred for 2 h at room temperature and further refluxed for 8 h. The product was poured into methanol (100 ml), and the precipitated product was filtered with filter paper, extracted in a soxhlet extractor with methanol for 8 h, and dried in vacuum (Zong, Kimura, Takahashi, & Yamane, 2000).

2.3. FT-IR spectroscopy

The IR spectra of CS, CMCS, and OCMCS were recorded on an FT-IR-430 Fourier Transform Infrared Spectrometer (Jasco Co., Tokyo, Japan) at room temperature based on the method of Shigemasa, Matsuura, Sashiwa, and Saimoto (1996). A pellet was formed from 2 mg samples and 100 mg of KBr.

2.4. Solubility test of OCMCS

Solubility of the OCMCS was evaluated from the turbidity (Kubota, Tatsumoto, Sano, & Toya, 2000). The pH dependence of the water solubility of CS, CMCS, and OCMCS was estimated from measurement of transmittance of the solution. Briefly, sample (10 mg) was dissolved in 2% (v/v) HCl solution (5 ml), the pH of the solution was adjusted by the addition of 10% NaOH solution and the transmittance of the solution at 600 nm as a function of pH value was recorded.

2.5. Erythrocyte toxicity assay

The hemolytic activities assay of OCMCS was conducted as described by Lee, Powers, and Baney (2004). Whole blood was obtained from two healthy male adults (22–30). 8 ml human blood was diluted with 10 ml normal saline. CS solution (0.2%) was prepared in the normal saline–acetic acid solution (Jumaa, Furkert, & Muller, 2002). CMCS and OCMCS solution (0.2%) was prepared in the normal saline. 10 ml such solution was added to the empty tubes. In brief, diluted blood (0.2 ml) was added to each sample that had been equilibrated in normal saline for 30 min at 37 °C and then all the tubes were incubated for 0.5, 1, and 2 h at 37 °C in a shaking water bath. The release of hemoglobin was determined after centrifugation (700 × *g* for 10 min) by photometric analysis of the supernatant at 545 nm.

Distilled water (100% hemolysis) and normal saline (0% hemolysis) were used as positive and negative controls for this work, respectively, and they were treated in the same way as previously. The hemolysis rate (HR) was calculated as follows:

$$\mathrm{HR} = \frac{\mathrm{Dt} - \mathrm{Dnc}}{\mathrm{Dpc} - \mathrm{Dnc}} \times 100\% \quad (1)$$

where Dt, Dnc and Dpc are the absorbance of the sample, the negative control and the positive control, respectively. The experiments were run in triplicate and were repeated twice.

2.6. The aggregation behavior of OCMCS

Pyrene was used as hydrophobic probe. Purified pyrene was dissolved in ethanol at the concentration of 0.4 mg/ml. About 10 μl of this solution was pipetted into a test tube, and the ethanol was driven off by under a stream of nitrogen gas. 10 ml of CS or OCMCS solution was added to the test tube, bringing the final concentration of pyrene to 2 μM. The mixture was incubated for 3 h in a water bath at 65° C and shaken in a BS-10 shaking water bath overnight at 20° C. Pyrene emission spectra were obtained using a Shimadzu RF-5301PC fluorescence spectrophotometer (Shimadzu Co., Kyoto, Japan). The probe was excited at 343 nm, and the emission spectra were collected in the range of 360–500 nm at an integration time of 1.0 s. The excitation and emission slit opening were 15 and 1.5 nm, respectively.

2.7. Preparation of OCMCS nanoparticles

20 mg of OCMCS was dissolved in 10 ml distilled water. Methylene chloride (3%, v/v) was added to the solution with stirring and homogenized (5 min, 13,000 × *g*) with an Ultra-Turrax T-25 dispersing machine. The solution was held under vacuum for 30 min to remove methylene chloride and then 1 ml of 0.25% sodium tripolyphosphate (STPP) solution was added as a crosslinking reagent. The rifampicin loaded nanoparticles was prepared by dissolving rifampicin in methylene chloride and subsequently emulsifying as above described.

The morphology of the OCMCS nanoparticles was observed by TEM with a JEM-2010. Solution of samples was placed onto a copper grill covered with nitrocellulose. They were dried at room temperature and then were examined using TEM by negative staining with an aqueous solution of sodium phosphotungstate.

The size distribution of nanoparticles was measured by the dynamic light scattering (DLS) with a Zetasizer 3000. All DLS measurements were done with a wavelength of 632.8 nm at 23° C.

2.8. Evaluation of in vitro drug release

The rifampicin loaded nanoparticles was prepared by dissolving rifampicin in methylene chloride and subsequently as described to prepare blank nanoparticles.

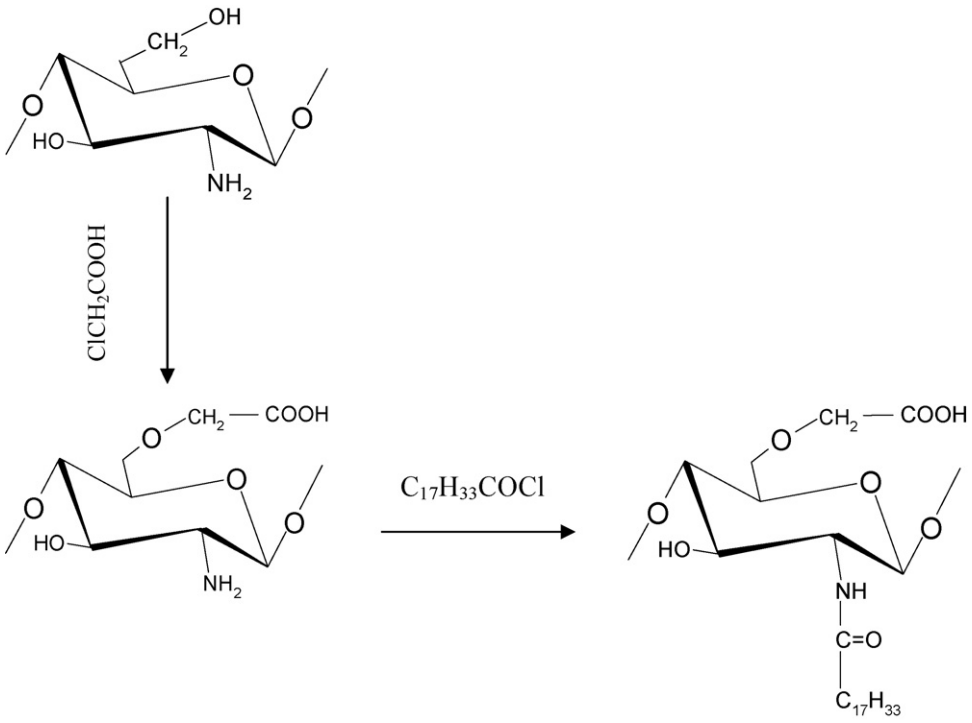

Fig. 1. Synthetic procedure of OCMCS.

In vitro release profile of rifampicin from the OCMCS nanoparticles was examined at 37 °C in a different release medium (acetate-buffer solutions pH 3.8, and phosphate-buffered saline PBS pH 6.8) for 36 h under protection from light. A cellulose membrane (8000–14,000) tube containing 2 ml of the rifampicin loaded OCMCS nanoparticles solution was placed in 100 ml of acetate-buffer or PBS at 37° C under protection from light. Incubations were carried out in a water bath at 37° C under gentle stirring. Periodically, the whole media was removed and replaced with fresh media to maintain sink conditions. The amount of released rifampicin was assayed by spectrophotometry at 475 nm in comparison to the standard curve.

The drug entrapment efficiency (EE) was calculated from the ratio of the drug amount in the nanoparticles to the total drug amount added in the solution. And the drug loading efficiency (LE) was calculated from the ratio of the drug amount in the nanoparticles to the weight of drug loaded nanoparticles.

2.9. Statistical analyses

The assays were performed at least in triplicate on separate occasions. The data collected in this study were expressed as the mean value ± standard deviation.

3. Results and discussion

3.1. Preparation and characterization of OCMCS

The synthetic scheme of OCMCS is represented in Fig. 1. There were hydrophilic and hydrophobic group on OCMCS chains. The introduction of hydrophobic group made it an amphiphilic molecule. And the introduction of hydrophilic group could improve the solubility.

The infrared spectra of CS, CMCS, and OCMCS are shown in Fig. 2. The basic characteristics of CS (Fig. 2a) at: 3455 cm^{-1} (O–H stretch), 2900 cm^{-1} (C–H stretch), 1596 cm^{-1} (N–H bend), 1154 cm^{-1} (bridge –O– stretch), and 1094 cm^{-1} (C–O stretch).

Compared to the spectrum of CS, the IR of CMCS (Fig. 2b) at 1740 cm^{-1} (–COOH), 1070–1136 cm^{-1} (–C–O–) and 1059 cm^{-1} (C–O–C) became stronger.

Compared to the IR spectrum of CMCS, the characteristic absorption of OCMCS (Fig. 2c) at 3200–3500 cm^{-1} (–OH, $-NH_2$) became weaker, the vibrational band corresponding to primary amino groups at 1570 cm^{-1} decreased. The peaks at 2924 cm^{-1} (δ=CH_2), 2854 cm^{-1} (δ=CH_2), 1464 cm^{-1} (δ=CH_2), 1182 cm^{-1} (twisting vibration of CH_2) were stronger and shaper in the latter. After oleoylation of CMCS, the spectra of OCMCS exhibited alterations compared to CMCS. These results confirmed that the CMCS had substituted with oleoyl chloride.

3.2. Solubility of OCMCS

The solubility of CS, CMCS, and OCMCS in aqueous solution is shown in Fig. 3. CS is soluble in aqueous acidic solution below pH 6.5 (Mao et al., 2004). The solubility of CS is caused by the protonation of primary amino groups ($-NH_2$). However, the applications

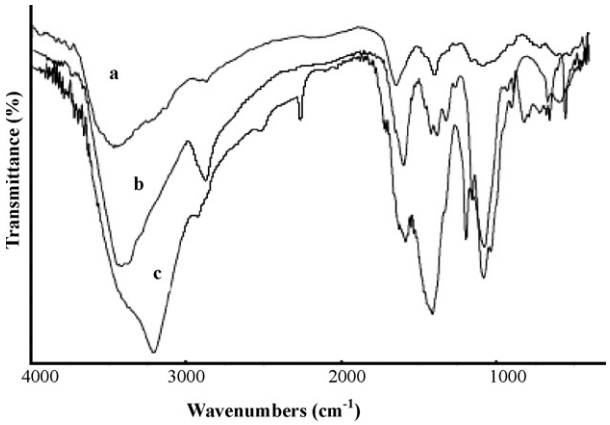

Fig. 2. The FT-IR spectra of (a) CS; (b) CMCS; (c) OCMCS.

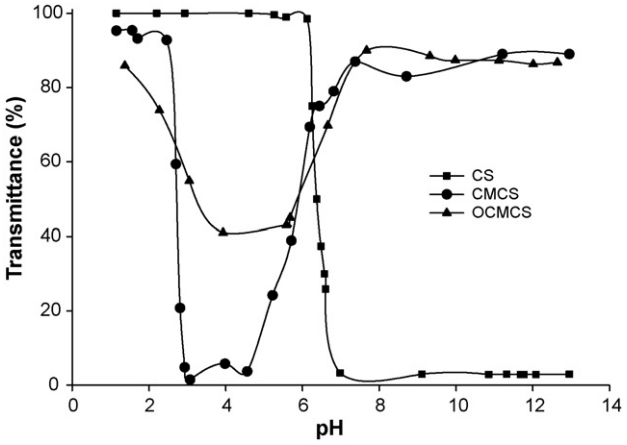

Fig. 3. Solubility of CS, CMCS, and OCMCS.

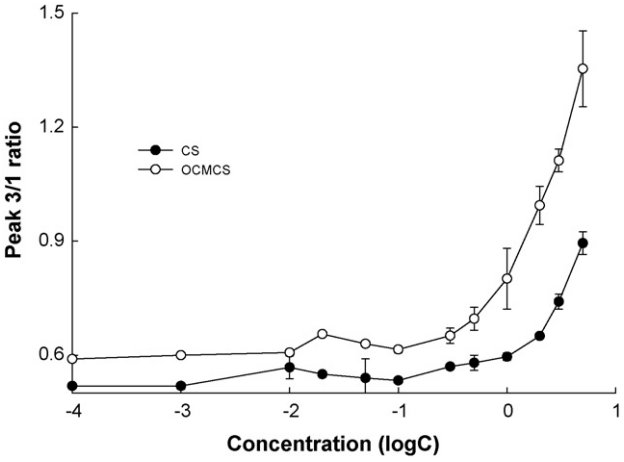

Fig. 5. Peak I_3/I_1 ratio of pyrene fluorescence as a functional of CS and OCMCS.

of chitin and chitosan in biology, in which many enzyme assays are performed at neutral pH, is quite restricted, because they are essentially insoluble in neutral water.

It could be seen from Fig. 3 the solubility property of OCMCS was similar with CMCS. OCMCS and CMCS were soluble in neutral solution. The solubility of CMCS and OCMCS in neutral water was due to the carboxymethylation of CS introduced carboxymethyl (–COOH) groups to CS. The improvement of solubility made their biological and physiological applications to develop dramatically.

3.3. Biocompatibility of OCMCS

Hemolysis of the blood is an important problem associated with the bio-incompatibility of materials. Red blood cell (RBC) hemolyse when come in contact with water. In vitro erythrocyte induced hemolysis is considered to be a simple and reliable measure for estimating blood compatibility of materials. Previously, the blood compatibility of unmodified CS in microspheres and emulsions was evaluated in terms of hemolysis (Remunan-Lopez & Bodmeier, 1996; Richardson, Kolbe, & Duncan, 1999). In this work, hemolysis was used to evaluate the biocompatibility of amphiphilic OCMCS.

Hemolysis results of human fresh blood with CS, CMCS, and OCMCS are shown in Fig. 4. The hemolysis rate (HR) of CS after 0.5, 1, and 2 h was 4.50%, 4.90% and 4.70%, respectively. The HR of CMCS after 0.5, 1, and 2 h was 0%, 1.35% and 2.00%, respectively. The HR of OCMCS after 0.5, 1, and 2 h was 2.34%, 7.11% and 8.00%, respectively. HR of CS was lower than 5%. The CMCS showed a negligible hemolysis (lower than 2%). However, the HR of OCMCS was a little higher than 5%, showing a certain level of red blood cell toxicity with it.

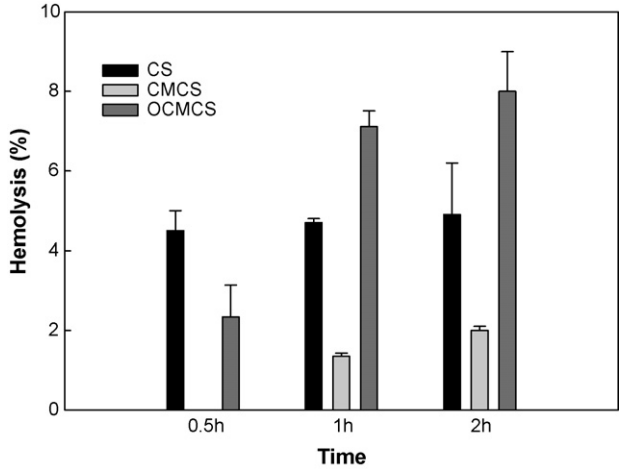

Fig. 4. Hemolysis of CS, CMCS, and OCMCS.

HR of CMCS was lower than CS. That could be explained from two aspects. On one hand, CS is a polysaccharide with amino groups which bears positive charges ($-NH_3^+$) in the physiological environment. That could act with some RBC which bears negative charges on surface. It was reported in previous papers that carboxymethylation reaction took place not only on the 6-O position but also on the 2-C and $-NH_2$ positions, which was reported in an earlier study (Chen & Park, 2003), so the carboxymethyl occupied some $-NH_2$. The decrease of $-NH_2$ could reduce the effect. The solubility of CMCS could improve the effect. On the other hand, the CMCS bears negative charges ($-COO^-$), which could release or avoid the electrostatic interaction between CMCS and cell membrane.

The HR of OCMCS was higher than CS and CMCS. That could be explained from several aspects. The high cationic charge densities and highly flexible polymers may cause higher cytotoxic effects. The long hydrophobic oleoyl groups on the surface of OCMCS may damage RBC, leading to enhanced release of hemoglobin. And the surface tension of OCMCS may also increase the damage. The results were consistent with an earlier study by Lee et al. (2004). However, the largest observed hemolytic activity was lower than 10%, which indicates a wide biocompatible margin in blood-contacting applications and suitability for intravenous administration (Jumaa et al., 2002).

3.4. Self-aggregates of OCMCS in solution

For fluorescence spectra measurement, CS was dissolved in 1% (v/v) acetic acid solution and OCMCS was dissolved in distilled water. Each spectrum corresponded to samples concentration of 0.0001–5 g/L. The variation of I_3/I_1 (I_{382}/I_{373}) ratio with the logarithm of concentration of CS and OCMCS is shown in Fig. 5. The peak I_3/I_1 ratio can therefore be used to determine the reactivity or aggregation properties of amphipathic molecules to the change in environment hydrophobicity in the aqueous system. The critical aggregation concentration (CAC) of samples was determined from the change of the quotient of vibrational band intensities in fluorescence emission spectrum of pyrene in a conventional way (Amiji, 1995).

The CAC value of OCMCS was 45.6 mg/L. The hydrophobic oleoyl chain substitutions in the macromolecule of OCMCS may facilitate its self-aggregation, favoring hydrophobic interactions and thus, the formation of dense polymer aggregates. And the large space

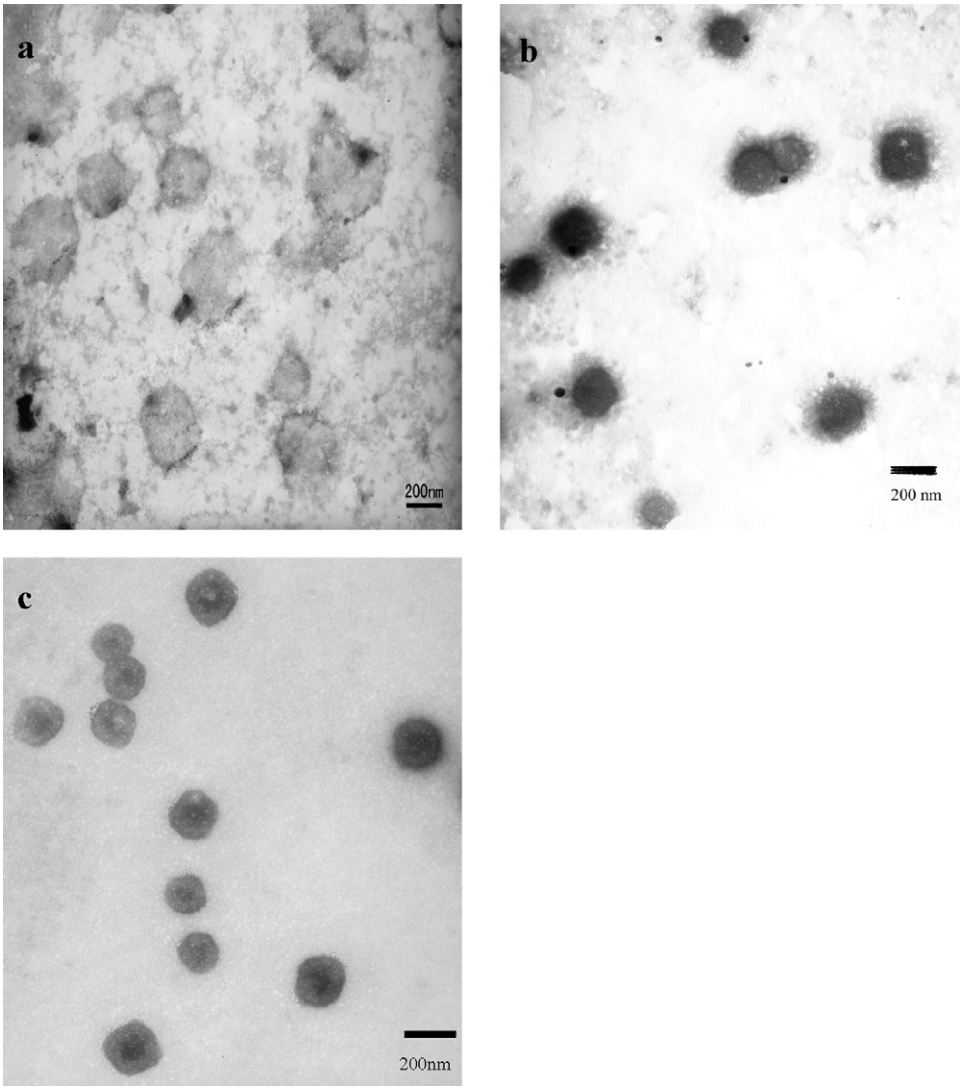

Fig. 6. TEM photographs of OCS and OCMCS nanoparticles (a) OCS (30,000×); (b) OCMCS (25,000×); (c) OCMCS (30,000×).

steric effect after modification is also a vital factor that should be taken into account.

The CAC value of OCMCS was much lower than that of a typical monomer surfactant SDS (sodium dodecyl sulphate) (2.1×10^3 mg/L) (Dominguez, Fernandez, Gonzalez, Iglesias, & Montenegro, 1997) and almost equivalent to those CAC of dodecyl-disaccharides based surfactants (86.7 mg/L) (Izawa et al., 1993).

3.5. TEM of OCMCS nanoparticles

The morphology of OCMCS nanoparticles was investigated by the transmission electron microscopy method. The TEM photographs of OCMCS nanoparticles were shown in Fig. 6. OCS nanoparticles prepared in our previous work (Li et al., 2007) are also shown in Fig. 6 to compare with OCMCS. The OCMCS nanoparticles were spherical in shape. The morphology of OCMCS nanoparticles was more regular and compact than OCS nanoparticles.

Hence, we could suggest that the introduction of carboxymethyl and oleoyl chain to CS might facilitate the formation of nanoparticles. One hand, the behavior of OCMCS in solution could be controlled by the ratio of the hydrophobic to the hydrophilic groups. We could adjust the ratio of hydrophobic to the hydrophilic groups to get an ideal proportion which could form ideal nanoparticles. On the other hand, the introduction of carboxymethyl improved the solubility of CS which made CS have a wide range of uses in the biotechnology and pharmaceutical fields.

Previously, the effect of degree of substitution (DS) of deoxycholic acid modified glycol chitosan to formation nanoparticles, size distribution, and stability of self-aggregates in aqueous media was evaluated by Kim et al. (2005). The formation of OCMCS nanoparticles might be affected by the DS of carboxymethyl and oleoyl. There existed an optimal DS and proportion of the hydrophobic and the hydrophilic groups.

3.6. Size distribution

Fig. 7 shows the size distribution of the nanoparticles formed by OCMCS. Mean diameter of the OCMCS nanoparticles was 161.8 nm. In our previous work we have known that the majority number of the OCS nanoparticles was around 275.3 nm in size. The size of self-aggregates decreased as the introduction of carboxymethyl, indicating formation of more dense hydrophobic cores in OCMCS.

3.7. In vitro release of rifampicin from OCMCS nanoparticles

The drug entrapment efficiency (EE) of the sample (rifampicin concentration 20 mg/ml and STPP 0.6%) was 39.9% and the loading efficiency (LE) was 19.95%.

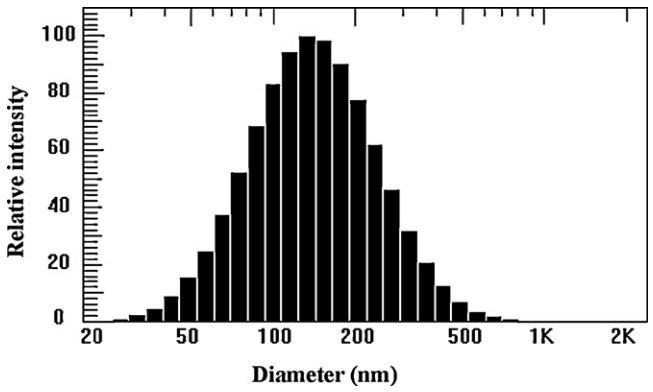

Fig. 7. Size distribution of OCMCS nanoparticles.

The rifampicin release profiles from OCMCS nanoparticles in acetate-buffer solutions (pH 3.8) and phosphate-buffer saline (pH 6.8) values are shown in Fig. 8. The nanoparticles might act as a barrier against the release of physically entrapped rifampicin after hydrolysis and the migration of rifampicin to release media might be strongly restricted by the hydrophobic core of the nanoparticles. The rifampicin release rate from OCMCS nanoparticles in phosphate-buffer saline (pH 6.8) was slower than that in acetate-buffer solutions (pH 3.8). We believed this was because when the pH value was 3.8, OCMCS self-assembled nanoparticles absorbed water to swell due to the ionization of amino groups, which resulting in the increase of permeability of their non-covalently crosslinked hydrogel structures, so that the rifampicin release rate increased accordingly (Wang et al., 2008). The other reason was the electrostatic interaction was greatly influenced by solutions' pH (Son et al., 2003). The decrease of pH weakened salt bonds and therefore, facilitated fiber swelling. So, the drug release was accelerated. And the medium pH also affected the micellization of the polymers (Cai & Jiang, 2009). The similar drug release mechanism from other pH-sensitive hydrogel systems has already been reported (Son et al., 2003; Wang, Dong, Du, & Kennedy, 2007).

In order to improve the stability of micelle and reduce the loss of drug in future in vivo transport process, the effects of crosslinking degree by STPP on the drug release behavior were investigated. The influence of crosslinker STPP on drug release in vitro is shown in Fig. 9. We could see that the addition of STPP could slower the

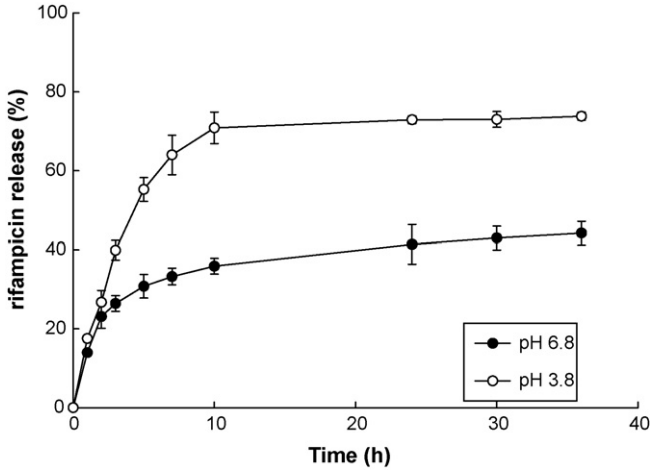

Fig. 8. Mean percent drug release from rifampicin loaded OCMCS nanoparticles in different pH values release medium; (○) release in pH 3.8 medium; (●) release in pH 6.8 medium (rifampicin concentrations 20 mg/ml and STPP 0.6%) (data shown are the mean ± S.D., $N = 3$).

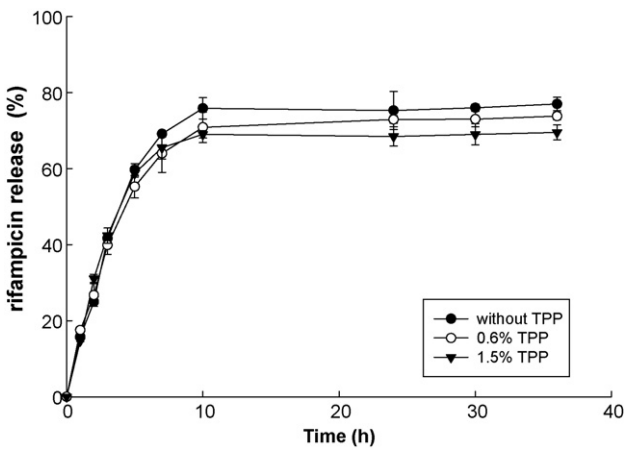

Fig. 9. Mean percent drug release from rifampicin loaded OCMCS nanoparticles with different STPP concentrations; (●) without STPP; (○) STPP 0.6%; (▼) STPP 1.5% (pH 3.8 and rifampicin concentrations 20 mg/ml) (data shown are the mean ± S.D., $N = 3$).

release of rifampicin. And the release rate of samples with more STPP was slower than that of with less STPP. The reason might be that the addition of STPP made the nanoparticles more stable and the connecting network was then formed from the percolation of bridges leading to a slowly release.

In summary, OCMCS could be synthesized by reacting CMCS with oleoyl chloride. The solubility, biocompatibility, formation of nanoparticles, and size of nanoparticles were affected by the proportion of the hydrophobic and the hydrophilic groups. We believe through adjusting the structure of the amphiphilic copolymers (the ratio of hydrophobic group to hydrophilic group), a kind of ideal water-soluble and biocompatible OCMCS could be prepared. And the size and morphology of the OCMCS micelles may be easily controlled.

4. Conclusion

OCMCS was synthesized by reacting CMCS with oleoyl chloride. The FT-IR results suggested the formation of an amide linkage between amino groups of CMCS and carboxyl groups of oleoyl chloride. The OCMCS exhibited good solubility in aqueous solution than CS. The CS was not soluble while the OCMCS and CMCS could be soluble at neutral pH. All the CS, CMCS, and OCMCS had good biocompatibility based on the results of the erythrocyte toxicity assay. Formation of self-aggregation was observed by use of pyrene as a fluorescent probe in the OCMCS aqueous solution. Nanoparticles were prepared using an o/w emulsification method. The morphology of OCMCS nanoparticles was more regular than OCS nanoparticles. Mean diameter of the OCMCS nanoparticles was 161.8 nm. Rifampicin, as a model drug, was investigated for its release properties in vitro. The addition of crosslinker STPP could slower the release of rifampicin. The rifampicin release rate was sensitive to the pH of the release media, because the electrostatic interaction, ionization, and micellization were greatly influenced by solutions' pH.

Acknowledgements

The authors are indebted to the financial support from NSFC (30670566), ISTCP (2006DFA33150).

References

Amiji, M. M. (1995). Pyrene fluorescence study of chitosan self-association in aqueous solution. *Carbohydrate Polymers*, *26*, 211–213.

Cai, G. Q., & Jiang, H. L. (2009). pH-sensitive nanoparticles self-assembled from a novel class of biodegradable amphiphilic copolymers based on chitosan. *Journal of Materials Science. Materials in Medicine*, *20*, 1315–1320.

Chen, X. G., Lee, C. M., & Park, H. J. (2003). O/W emulsification for the self-aggregation and nanoparticle formation of linoleic acid-modified chitosan in the aqueous system. *Journal of Agricultural and Food Chemistry*, *51*, 3135–3139.

Chen, X. G., & Park, H. J. (2003). Chemical characteristics of *O*-carboxymethyl chitosans related to the preparation conditions. *Carbohydrate Polymers*, *53*, 355–359.

Dominguez, A., Fernandez, A., Gonzalez, N., Iglesias, E., & Montenegro, L. (1997). Determination of critical micelle concentration of some surfactants by three techniques. *Journal of Chemical Education*, *74*, 1227–1230.

Garcia-Fuentes, M., Prego, C., Torres, D., & Alonso, M. J. (2005). A comparative study of the potential of solid triglyceride nanostructures coated with chitosan or poly(ethylene glycol) as carriers for oral calcitonin delivery. *European Journal of Pharmaceutical Sciences*, *25*, 133–143.

Gupta, K. C., & Jabrail, F. H. (2006). Glutaraldehyde and glyoxal cross-linked chitosan microspheres for controlled delivery of centchroman. *Carbohydrate Research*, *341*, 744–756.

Izawa, S., Sakai-Tomita, Y., Kinomura, K., Kitazawa, S., Tsuda, M., & Tsuchiya, T. (1993). Introduction of a series of alkyl thiomaltosides, useful new non-ionic detergents, to membrane biochemistry. *Journal of Biochemistry*, *113*, 573–576.

Jumaa, M., Furkert, F. H., & Muller, B. W. (2002). A new lipid emulsion formulation with high antimicrobial efficacy using chitosan. *European Journal of Pharmaceutics and Biopharmaceutics*, *53*, 115–123.

Kakizawa, Y., Harada, A., & Kataoka, K. (2001). Glutathione-sensitive stabilization of block copolymer micelles composed of antisense DNA and thiolated poly(ethyleneglycol)-block-poly(L-lysine): A potential carrier for systemic delivery of antisense DNA. *Biomacromolecules*, *2*, 491–497.

Kim, J. H., Kim, Y. S., Kim, S., Park, J. H., Kim, K., Choi, K., et al. (2006). Hydrophobically modified glycol chitosan nanoparticles as carriers for paclitaxel. *Journal of Controlled Release*, *111*, 228–234.

Kim, K., Kwon, S., Park, J. H., Chung, H., Jeong, S. Y., & Kwon, I. C. (2005). Physicochemical characterizations of self-assembled nanoparticles of glycol chitosan-deoxycholic acid conjugates. *Biomacromolecules*, *6*, 1154–1158.

Kim, Y. H., Gihm, S. H., & Park, C. R. (2001). Structural characteristics of size-controlled self-aggregates of deoxycholic acid-modified chitosan and their application as a DNA delivery carrier. *Bioconjugate Chemistry*, *12*, 932–938.

Koziara, J. M., Whisman, T. R., Tseng, M. T., & Mumper, R. J. (2006). In-vivo efficacy of novel paclitaxel nanoparticles in paclitaxel-resistant human colorectal tumors. *Journal of Controlled Release*, *112*, 312–319.

Kubota, N., Tatsumoto, N., Sano, T., & Toya, K. (2000). A simple preparation of half *N*-acetylated chitosan highly soluble in water and aqueous organic solvents. *Carbohydrate Research*, *324*, 268–274.

Lee, D. W., Powers, K., & Baney, R. (2004). Physicochemical properties and blood compatibility of acylated chitosan nanoparticles. *Carbohydrate Polymers*, *58*, 371–377.

Li, F., Liu, W. G., & Yao, K. D. (2002). Preparation of oxidized glucose cross-linked *N*-alkylated chitosan membrane and in vitro studies of pH-sensitive drug delivery behaviour. *Biomaterials*, *23*, 343–347.

Li, Y. Y., Chen, X. G., Liu, C. S., Cha, D. S., Park, H. J., & Lee, C. M. (2007). Effect of the molecular mass and degree of substitution of oleoylchitosan on the structure, rheological properties, and formation of nanoparticles. *Journal of Agricultural and Food Chemistry*, *55*, 4842–4847.

Liu, C. G., Desai, K. G. H., Chen, X. G., & Park, H. J. (2005). Linolenic acid-modified chitosan for formation of self-assembled nanoparticles. *Journal of Agricultural and Food Chemistry*, *53*, 437–441.

Liu, C. G., Fan, W. W., Chen, X. G., Liu, C. S., Meng, X. H., & Park, H. J. (2007). Self-assembled nanoparticles based on linoleic-acid modified carboxymethyl-chitosan as carrier of adriamycin (ADR). *Current Applied Physics*, *7*, 125–129.

Liu, X. F., Guan, Y. L., Yang, D. Z., Li, Z., & Yao, K. D. (2001). Antibacterial action of chitosan and carboxymethylated chitosan. *Journal of Applied Polymer Science*, *79*, 1324–1335.

Mao, S. R., Shuai, X. T., Unger, F., Simon, M., Bi, D. Z., & Kissel, T. (2004). The depolymerization of chitosan: Effects on physicochemical and biological properties. *International Journal of Pharmaceutics*, *281*, 45–54.

Martin, L., Wilson, C. G., Koosha, F., Tetley, L., Gray, A. I., Senel, S., et al. (2002). The release of model macromolecules may be controlled by the hydrophobicity of palmitoyl glycol chitosan hydrogels. *Journal of Controlled Release*, *80*, 87–100.

Park, J. H., Kwon, S., Lee, M., Chung, H., Kim, J. H., Kim, Y. S., et al. (2006). Self-assembled nanoparticles based on glycol chitosan bearing hydrophobic moieties as carriers for doxorubicin: In vivo biodistribution and anti-tumor activity. *Biomaterials*, *27*, 119–126.

Remunan-Lopez, C., & Bodmeier, R. (1996). Effect of formulation and process variables on the formation of chitosan–gelatin coacervatives. *International Journal of Pharmaceutics*, *135*, 63–72.

Richardson, S. C. W., Kolbe, H. V. J., & Duncan, R. (1999). Potential of low molecular mass chitosan as a DNA delivery system: Biocompatibility, body distribution and ability to complex and protect DNA. *International Journal of Pharmaceutics*, *178*, 231–243.

Shigemasa, Y., Matsuura, H., Sashiwa, H., & Saimoto, H. (1996). Evaluation of different absorbance ratios from infrared spectroscopy for analyzing the degree of deacetylation in chitin. *International Journal of Biological Macromolecules*, *18*, 237–242.

Son, Y. J., Jang, J. S., Cho, Y. W., Chung, H., Park, R. W., Kwon, I. C., et al. (2003). Biodistribution and anti-tumor efficacy of doxorubicin loaded glycol-chitosan nanoaggregates by EPR effect. *Journal of Controlled Release*, *91*, 135–145.

Wang, Q., Dong, Z. F., Du, Y. M., & Kennedy, J. F. (2007). Controlled release of ciprofloxacin hydrochloride from chitosan/polyethylene glycol blend films. *Carbohydrate Polymers*, *69*, 336–343.

Wang, Y. S., Jiang, Q., Li, R. S., Liu, L. L., Zhang, Q. Q., Wang, Y. M., et al. (2008). Self-assembled nanoparticles of cholesterol-modified *O*-carboxymethyl chitosan as a novel carrier for paclitaxel. *Nanotechnology*, *19*, 102–201.

Wu, Y., Zheng, Y. L., Yang, W. L., Wang, C. C., Hu, J. H., & Fu, S. K. (2005). Synthesis and characterization of a novel amphiphilic chitosan–olylactide graft copolymer. *Carbohydrate Polymers*, *59*, 165–171.

Xu, Y. M., & Du, Y. M. (2003). Effect of molecular structure of chitosan on protein delivery properties of chitosan nanoparticles. *International Journal of Pharmaceutics*, *250*, 215–226.

Zhang, C., Ping, Q. N., Zhang, H. J., & Shen, J. (2003). Preparation of *N*-alkyl-*O*-sulfate chitosan derivatives and micellar solubilization of taxol. *Carbohydrate Polymers*, *54*, 137–141.

Zong, Z., Kimura, Y., Takahashi, M., & Yamane, H. (2000). Characterization of chemical and solid state structures of acylated chitosans. *Polymer*, *41*, 899–906.